Quaternary Science Advances 12 (2023) 100103

Contents lists available at ScienceDirect

Quaternary Science Advances

journal homepage: www.sciencedirect.com/journal/quaternary-science-advances

A steady-state model reconstruction of the patagonian ice sheet during the last glacial maximum

Ingo W. Wolff [a], Neil F. Glasser [a,*], Stephan Harrison [b], Joanne Laura Wood [b], Alun Hubbard [c,d]

[a] Department of Geography and Earth Sciences, Aberystwyth University, Wales, SY23 3DB, UK
[b] Centre for Geography and Environmental Science, University of Exeter, Penryn Campus, Penryn, Cornwall, TR10 9FE, UK
[c] IC3 – Centre for Ice, Climate, Carbon & Cryosphere, Institutt for Geosciences, UiT - the Arctic University of Norway, Tromsø, N-9037, Norway
[d] Geography Research Unit, Oulun Yliopisto, Oulu University, Oulu, F-90570, Finland

A B S T R A C T

During the Last Glacial Maximum (LGM), the Patagonian Ice Sheet (PIS) was the largest Quaternary ice mass in the Southern Hemisphere outside of Antarctica. Although the margins of the LGM ice sheet are now well established through end-moraine mapping and dating, apart from a few modelling and empirical studies, there remains a lack of constraint on its thickness and three-dimensional configuration. Here, we provide a high-resolution steady-state model reconstruction of the PIS at its maximum - LGM - extent applied using Nye's perfect-plastic ice rheology. The yield-strength parameter for the perfect-plastic flow model was calibrated against independent empirical reconstructions of the Lago Pueyrredón Glacier, where the former vertical extent of this major outlet glacier is well constrained by cosmogenically-dated trimlines and lateral and end-moraine limits. Using this derived yield-strength parameter, the perfect-plastic model is then applied to multiple flowlines demarking each outlet across the entirety of the PIS in a GIS framework. Our results reveal that the area of the PIS was ~504,500 km^2 (±8.5%) with a corresponding modelled ice volume of ~554,500 km^3 (±10%), equivalent to ~1.38 m (±10%) of eustatic sea-level lowering at the LGM. Maximum surface elevation was at least 3500m asl although the majority of the ice sheet surface was below 2500 m asl. We find that our ice sheet reconstruction is in good general agreement with previous estimates of net PIS volume derived from transient modelling studies. We attribute the slightly lower aspect-ratio of our ice sheet (and its concomitant 5% reduction in volume and sea-level equivalent) to the lower yield strength applied, based on more temperate and dynamic ice sheet conditions.

1. Introduction

Southern Patagonia is the only land mass on Earth that interacts with the Southern Westerly Wind Belt (SWWB) within the latitudinal band 47 to 55°S (Coronato et al., 2004; Kilian and Lamy, 2012; Lenaerts et al., 2014). As a result, it is a key location for reconstructing the behaviour of the SWWB and associated atmospheric and oceanic systems such as the Southern Annular Mode (SAM) during recent (e.g. Jones et al., 2016), earlier Holocene (e.g. Abram et al., 2014) and lateglacial times (eg Kilian and Lamy, 2012; Boex et al., 2013). As a mostly terrestrial ice sheet, the former Patagonian Ice Sheet (PIS) also offers an important opportunity to reconstruct former ice volumes and to determine its contribution to overall eustatic sea-level lowering of 125 m globally, at the LGM.

To the east of the contemporary icefields in Southern Patagonia are a series of moraine belts recording fluctuations of the Pleistocene Patagonian Ice Sheet over the last million years (Caldenius, 1932; Wenzens, 2005, 2006; Davies et al., 2020) and these represent some of the longest depositional records of glacier fluctuations on Earth (Kaplan et al., 2009). Given this, Patagonia offers a unique location for inferring global climate-system changes from past glacial chronologies such as changes in the position of the SWWB core (e.g. Warren and Sugden, 1993; Hulton and Sugden, 1997; Hulton et al., 2002; Sugden et al., 2002; Heusser, 2003; Darvill et al., 2015b; 2016) and questions concerning inter-hemispheric teleconnections of glacial fluctuations (e.g. Denton et al., 1999; McCulloch et al., 2000; Glasser et al., 2004, 2008; Sugden et al., 2005; Glasser et al., 2012).

The lateral extent of the PIS during the Last Glacial Maximum (LGM) was initially reconstructed by the mapping of Caldenius (1932). During this period (viewed as between 25,000–16,000 cal. yr. B.P. Rabassa et al., 2005; Rabassa (2008), the PIS stretched 2300 km or so from north to south perpendicular to the Southern Westerly Wind Belt (SWWB) (Clapperton, 1993; Glasser et al., 2008; Kaplan et al., 2008). While much is known of the horizontal extent of the PIS (e.g. Glasser and Jansson, 2005; Davies et al., 2020; Leger et al. 2021; García et al., 2021; Soteres et al., 2022), especially to the east of the current icefields, there are a number of clear gaps in our knowledge. First, there are very few constraints of its former vertical extent. Without the ice surface distribution, we are unable to answer questions about the nature of the climate forcing that drove the development of the PIS, nor can we track

* Corresponding author.
E-mail address: nfg@aber.ac.uk (N.F. Glasser).

https://doi.org/10.1016/j.qsa.2023.100103
Received 17 March 2023; Received in revised form 7 July 2023; Accepted 13 July 2023
Available online 17 July 2023

thickness changes of the PIS during deglaciation and in response to shifts in the precipitation-bearing SWWB. Only in the Lago Pueyrredon and Chacabuco Valley region of the NPI has the thickness of the PIS been assessed using dating and mapping of trimlines (Boex et al., 2013). Second, although the former margins of the PIS are well mapped and dated along its eastern extent, the positions of the western and southern margins are largely unknown and are likely to have been dominated by ice fronts calving into the Pacific during the LGM.

Given that the vast majority of published dates concentrate on establishing its limits at the LGM, we focus here on PIS extent during the LGM (see reviews of geomorphology and geochronology in Glasser et al., 2008; Glasser and Jansson, 2008; Davies et al., 2020). We also focus on the LGM for several reasons. This period represents the time when global ice extent and volume was greatest during the Last Glacial Cycle, and was a time when significant changes occurred in atmospheric and oceanic circulation occurred, with subsequent major impacts on terrestrial geological and ecological systems (Hughes, 2022). As a result, the LGM is the most important stage of the last glacial cycle in terms of unravelling former environmental, sea-level, climatic and geological footprint of the PIS. In addition, the LGM is the last period when the global climate was in an equilibrium state different from the present day climate and this means that the LGM has been used to test assumptions about climate sensitivity (e.g. Sherwood et al., 2020) and the ways in which climate models simulate climate responses to changes in radiative forcing (e.g. Annan et al., 2022).

The aims of this paper are:

1. To present a new assessment of the most likely vertical and horizontal extent of the PIS during the LGM;
2. To use this planiform shape as boundary conditions to model the three-dimensional configuration of the ice-sheet;
3. To calculate the former ice-sheet area and volume and its contribution to global sea-level change after the LGM.

1.1. Study area

The model domain covers 2300 km from 36°30′S to Cape Horn at 56°S and includes the Patagonian and Fuegian Andes and adjacent lowlands. The west-east distance of the area of ice-sheet reconstructions varies from less than 120 km in the north (38°S) to over 350 km around 46°S. We subdivide the area into three distinct sub-areas: A) the northern part of Patagonia including the Chilean Lake District from 36°30′to 44°18′S, B) extends down to 52°12′S covering the North and South Patagonian ice fields, and C) extends South to 56°S and covers Tierra del Fuego and the Cordillera Darwin Icefield (CDI) to the shelf off Cape Horn (see Fig. 1). The study region includes the three major ice fields, which represent the largest ice masses outside Antarctica in the Southern Hemisphere. These are the 4200 km^2 North Patagonian Icefield (NPI) from 46°30′S to 47°30′S; 73°W to 74°W; the 13000 km^2 South Patagonian Icefield (SPI) (48°30′S to 51°S; 73°W to 74°W, and the 2000 km^2 CDI from 54°30′S to 55° S; 69°W to 71°W (Warren and Sugden, 1993). Prominent mountain peaks include: Volcan Lanin (3777 m asl), Monte Tronador (3554 m a.s.l.), Monte San Valentin (3910 m asl and Monte San Lorenzo (3706 m asl).

2. Methods

Our study uses the following steps:

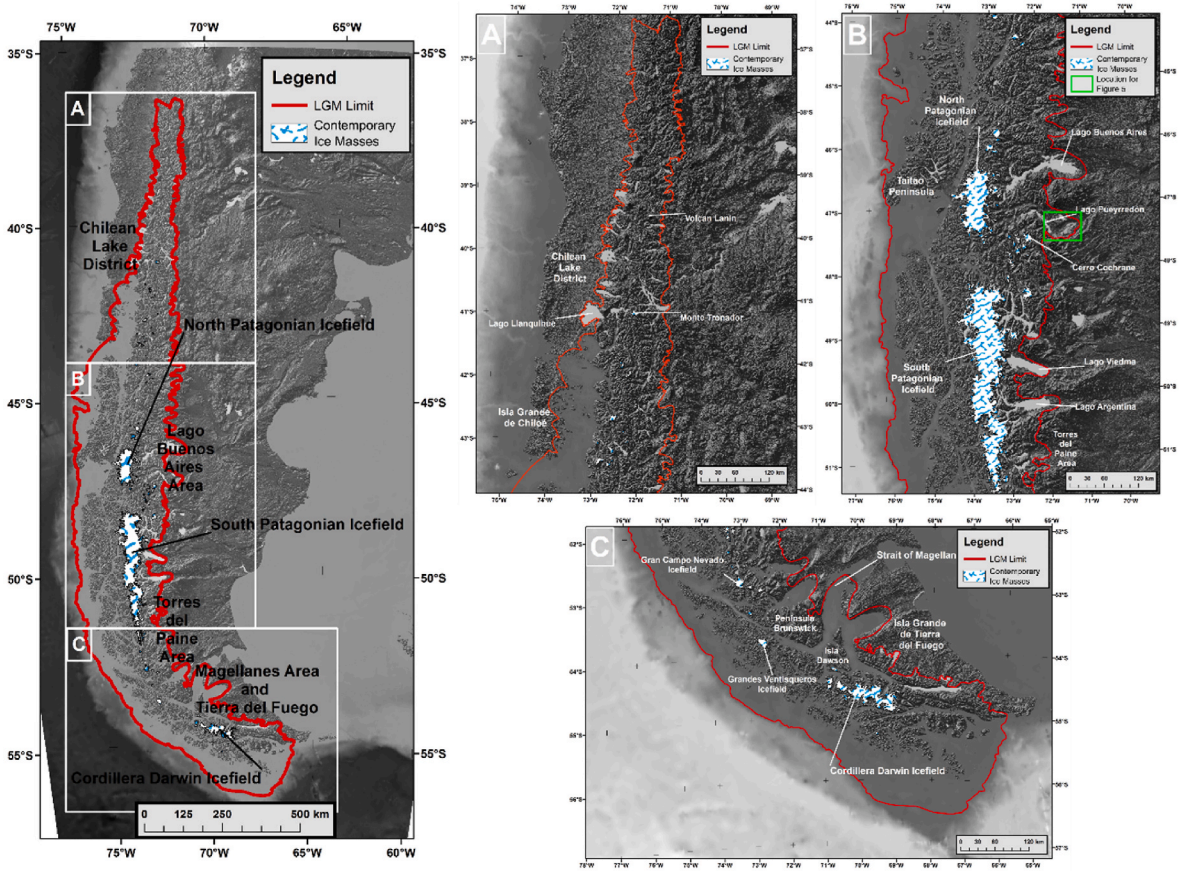

Fig. 1. Location map showing the outline of the Patagonian Ice Sheet at the Last Glacial Maximum (LGM) as well as areas mentioned in the text. The locations of contemporary ice masses are also shown.

- establish a spatio-chronological framework of dated locations from the literature and from the glacial geomorphological record within an integrated GIS database using high-resolution map data.
- create a likely LGM extent of the PIS from the spatio-chronological framework established by the integrated GIS database.
- develop and test a flow-line-based 3D glacier reconstruction on the small and independent Meseta Cuadrada palaeo ice cap (see Wolff et al., 2013), including application of ELA and glacier-accumulation reconstruction methods which can be used as a test of the method for the larger LGM PIS.
- creation of a 3D reconstruction of the LGM PIS using GIS with 100 m horizontal resolution and including volume estimates.

We apply a perfect-plastic ice rheology (Nye, 1952a, 1952b, 1957) to reconstruct the former PIS based on its known former extent. This approach gained wide-spread usage in the 1970s to reconstruct Quaternary ice masses (e.g. Hughes, 1979; Denton and Hughes, 1981). For ease of application, we embed the perfect-plastic model within a GIS framework that also includes the published and known ice limits from trimlines, lateral and end-moraines and includes reconstruction of the former extent of the PIS (see Wolff (2016) for full details). We use a perfect-plastic flowline approach for several reasons. First, it is computationally far more efficient than a higher-order time-dependent numerical ice-sheet model to produce a three-dimensional ice-sheet reconstruction. Forward integrated ice sheet models require palaeo-climate data to force mass-balance values and these data are lacking in Patagonia. Second, it fully embraces and honours the marginal ice-limits (where they are well established), which is a distinct advantage where the ice sheet has complex outlet configurations that impact on the overall ice sheet morphology.

Despite this, there are drawbacks and these include: 1) the approach assumes that the ice sheet is in steady-state; 2) the model assumes unvarying yield-strength parameters which can vary in space/time depending on changes in ice sheet dynamics/rheology; 3) the model does not account for any transient evolution of the ice sheet nor link to paleo-climate.

Despite these limitations, the use of the Nye (1957) perfect-plastic model for ice sheet reconstruction has undergone recent resurgence in its application due to its simplicity, computational efficiency and ease of application. Specifically it has been applied to reconstruct numerous valley glaciers, e.g. in Patagonia (Hubbard, 1997), but recently to reconstruct global ice sheets over the last glacial cycle (Gowan et al., 2021) and the Eurasian Ice Sheet during its LGM deglaciation (Sejrup et al., 2022).

In this study – to provide a more accurate and realistic calibration of the yield-strength parameter – the only variable in the model that broadly equates to ice viscosity, we apply the perfect-plastic model to a well-constrained case study where the vertical and horizontal limits are known from empirical evidence (Boex et al., 2013) before subsequently applying the model to the entire ice sheet.

The reconstruction of the PIS directly follows the methods presented in Wolff et al. (2013) and is further summarised here. The glacial geomorphology of the area covered by the PIS was depicted in ArcGIS using a scale between 1:20,000 and 1:10,000 based on georeferenced Google Earth imagery (about 3 m resolution derived by SPOT imagery) and additional ASTER DEM data for elevation control (30 m resolution) from NASA's REVERB/ECHO homepage (http://reverb.echo.nasa.gov/reverb/). The distinction between formerly glaciated areas and unglaciated areas is clear, as well as the identification of moraines, hummocky moraines, eskers, and ice-contact features.

Geomorphological mapping was undertaken following the guidelines developed by Glasser and Jansson (2008), and Glasser et al. (2008). Each landform was digitized within ArcGIS and added to a geodatabase of glacial landforms.

With the absence of an absolute chronology for large parts of the region we can only suggest the timing of the mapped moraine belts. Where timing is unknown, we used the broad hummocky outer moraine belts, which have a striking morphostratigraphic similarity with moraines from the 'Rio Blanco Limit' built up by the Lago Pueyrredón palaeo ice stream. Hein et al. (2009, 2010) assigned these similar looking moraines to the LGM.

Application requires accurate determination of former ice sheet extent and accurate topographic data to ensure that the modelled ice configuration is realistic, given the topographic complexity and large gradients across the Andes and hinterland regions covered by the PIS. To maintain the highest possible degree of reproducibility, we calculated the likely ice thickness along a dense array of glacier surface profiles using the approach of Nye (1952a) (see Figs. 2 and 3). Isostatic adjustment of the lithosphere beneath the LGM PIS was calculated based on the ice thickness, following the general observation that the isostatic depression beneath ice sheets generally mirrors the density ratio of ice to mantle bedrock.

The distance between each single surface profile ranges between $\leq$100 m in most parts of the ice sheet to $\geq$1000 m between the northern and southern ice sheet lobes. This array of glacier surface profiles produces a smooth surface during the later highlighted interpolation process within ArcGIS. Each surface profile consists of one data point counting upward each 100 m from the moraine position until the head boundary is reached. Each point contains the extracted ASTER DEM elevation, the distance to the moraine belt in 100 m steps, and an identification value assigned to the corresponding surface profile. Based on the original equation from Nye (1952) to calculate the shear stress of a parallel-slab geometry ice body

$$\tau_{xy} = -\rho g d\, dh/dx$$

with τ_{xy} as shear stress in kPa (kilo-Pascal), ρ the density of ice (920 kg/m3), g the gravitational constant (9.8 m/s2), d the ice thickness in metres and sinα as bed slope; a spreadsheet in EXCEL with a rearranged and adapted version of Nye's equation produced ice thickness values of each glacier profile. The insertion of bed elevation, point distance, and the widely accepted value of 90 kPa (0.9 bar) yield strength (Nye, 1952b; Schilling and Hollin, 1981) delivered the most realistic ice thickness values within the unconfined Meseta Cuadrada palaeo ice cap (see Wolff et al., 2013). Once the ice thickness was calculated, the new glacier surface elevation points were used to interpolate the surface of the palaeo ice sheet. For practical reasons merging the points of the glacier surface profiles with points of current elevation along the inferred glacier outline is useful, otherwise the interpolated surface is unconstrained. The interpolation procedure is done with ArcGIS Spatial Analyst, where the spline interpolation with a tension of 0.5–125 points delivers the best outputs in terms of yielding a comparatively smooth glacier surface without artifacts.

Once such a database of ice sheet margins is developed, the spatial relationship between distinct ice sheet extents can be used to extract general moraine system patterns from the LGM. These general moraine system patterns can then be used to infer undated moraines to the LGM.

3. Results

The dense and complex flow-line networks in the three regions are shown in Fig. 3. Development of these flow-line networks allowed the 3D reconstruction of the PIS. The reconstructions of the surface elevation of the PIS are shown in Fig. 4. The interpolated ice-sheet surface of the final LGM PIS reconstruction has a horizontal resolution of 100 m and measures ~504,500 km^2 ($\pm$8.5%) in area extent, and, therefore, is about 25% of the surface area of Greenland. The calculated volume of the interpolated ice body measures ca. 554,000 km^3 ($\pm$10%) and equates to a potential rise in sea level of 1.38 m ($\pm$10%) above present-day levels. The lack of bathymetry data for the large glacial lakes, except for Lago Buenos Aires, reduces the calculated volume to a certain degree, but compared to the overall volume, the likely effect of unknown

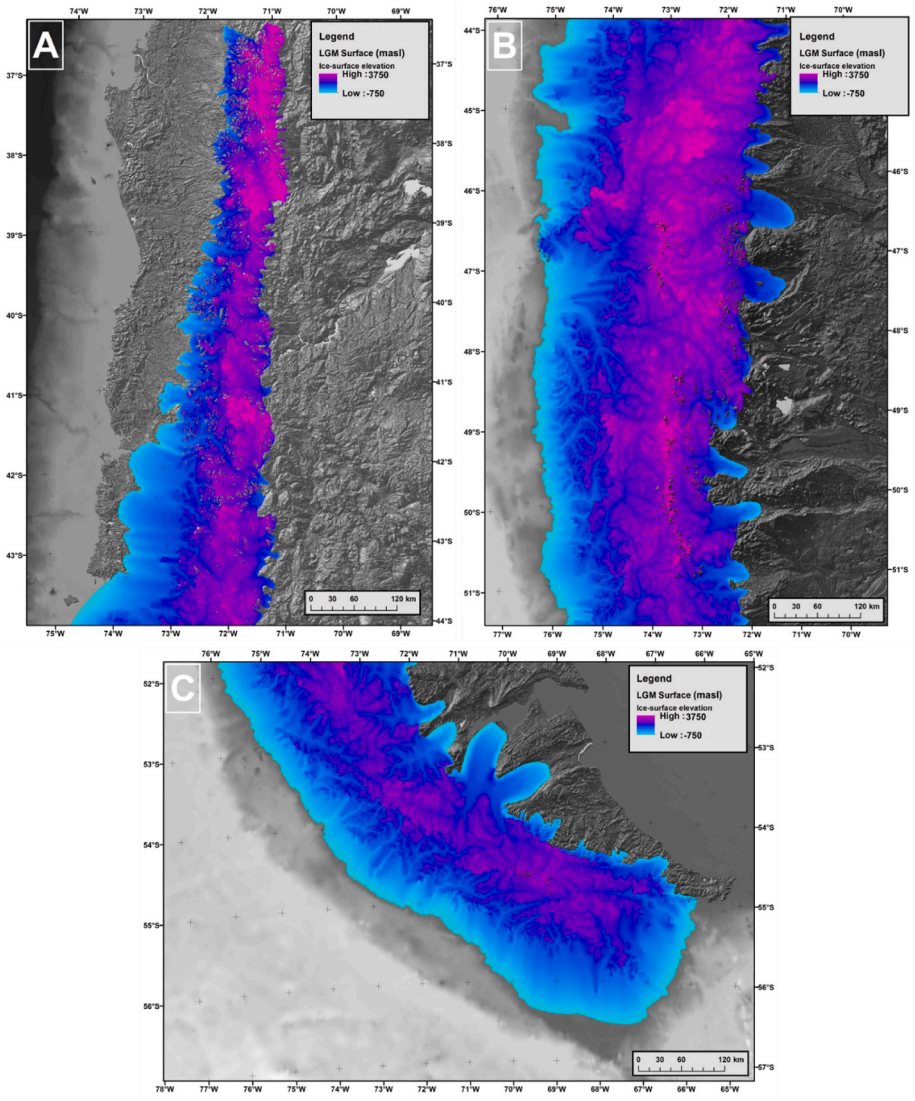

Fig. 2. The reconstructed Patagonian Ice Sheet surface at the Last Glacial Maximum.

lake volumes in the calculation is negligible.

While the reconstructed ice elevation reaches the height of the highest contemporary summits (i.e. ~3500m asl) most of the interpolated ice-surface elevation is lower than 2500 m asl, and has a mean elevation of ~1158 m asl. Only 0.68% of the ice-sheet area is higher than 2500 m asl. while the area with elevations above 2000 m asl. represents approximately 39% of the complete area.

The calculated maximum thickness of the ice-sheet, calculated to take account of isostatic adjustment, is around 3500 m and ice thicknesses above 3000 m are primarily found in the deep fjords west of the Patagonian Andes (see Fig. 4). Mean ice thickness is 1098 m and the mean surface slope of the complete ice-sheet is at ca. 3°. Fig. 4 shows the thickness of the interpolated ice-sheet and the LGM extent, which leads to significant ice thickness over the Islas Wollaston/Islas Hermite archipelago and south of Isla Navarino.

We have reconstructed ice thicknesses for the entire LGM PIS. However, testing these reconstructions using empirical data has not been possible in most parts of the PIS given the absence of data on its former vertical extent. Only in the region of the Lago Pueyrredón outlet lobe east of the Andes are data available from high elevation mountains to test ice thickness calculations. In this region we also have previous simulations of the outlet lobes (Hubbard et al., 2005; Kaplan et al., 2009, Fig. 5). Well developed lateral moraines and glacial-periglacial trimlines demonstrate the existent of palaeo-nunataks which existed above the former ice sheet surface. These are particularly well-developed in the vicinity of Sierra Colorado (and also on Cerro Tamango and Cerro Oportus to the west). These represent the only locations of the entire research area, where pre-LGM and LGM glacier trimlines and high-level lateral moraines have been successfully dated (Boex et al., 2013), thus providing insights into vertical elevation changes of the PIS. The Lago Pueyrredón outlet lobe remains the most important key location to validate the reconstructed ice-sheet thickness, even though the validation remains only locally valid (Fig. 5).

Our reconstructed LGM PIS surface aligns very closely to the 28,980 ± 1206 a B.P. dating locations on Sierra Colorada provided by Boex et al. (2013) (Fig. 5). The age of the higher-altitude moraines is 177,151 ± 7229 a B.P. The agreement between mapped and dated LGM moraines on the slopes of Sierra Colorada and the reconstructed 3D LGM ice-sheet surface supports our 3D reconstruction, at least in this region. This is the first time that this Sierro Colorada nunatak has been correctly reproduced in a reconstruction for the LGM PIS. A previous reconstruction of the extent of northern sector of the PIS by Hubbard et al. (2005), which yielded the best spatial resolution of an ice-sheet simulation at this location, does not yield this prominent nunatak protruding their modelled paleo-ice surface.

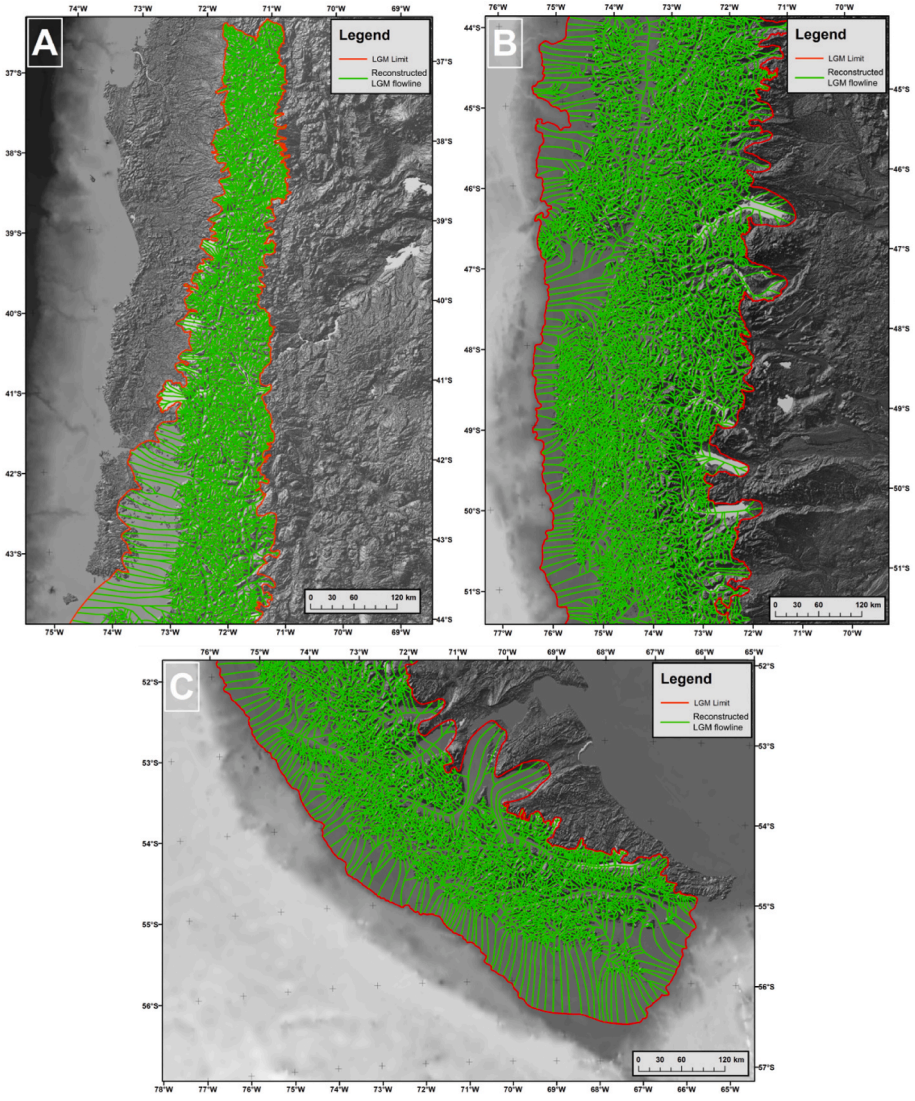

Fig. 3. Flowlines used to reconstruct the extent of the Patagonian Ice Sheet at the Last Glacial Maximum.

4. Discussion

There have now been a number of reconstructions of the volume of the LGM PIS. The volume of our newly reconstructed ice-sheet can be compared to the range of reconstructions by Hollin and Schilling (1981) and the modelling simulations of the LGM PIS by Hulton et al. (1994, 2002); Hulton and Sugden (1997).

The calculated ice volume of the reconstruction from this study of 554,000 km^3 is 214,000 km^3 higher than the volume of 340,000 km^3 produced by Hollin and Schilling (1981). Their volumetric estimate represents a sea-level equivalent of 0.85 m, which is considerably lower than the revised estimate presented in this study. It is also much larger than the volumetric estimate of Hulton et al. (1994) and Hulton and Sugden (1997), of 440,000 km^3. Later, Hulton et al. (2002) calculated the PIS at 481,333 km^3 producing a 1.2 m sea-level equivalent. The most recent reconstruction is that provided by Davies et al. (2020) who assessed ice volumes of the PIS at various time slices from 35ka to 2011 using volume-scaling estimates. Several relevant time slices from their study are shown in Table 1 along with other ice volume and sea level equivalent reconstructions.

The reconstruction of the LGM PIS presented in this paper is the only ice sheet reconstruction produced taking account of isostatic adjustment of the lithosphere and we suggest that the lack of isostatic adjustment may be one reason for the discrepancies between the ice volume of this study and previous reconstructions and simulations of the LGM PIS. Our initial ice sheet interpolation with the same yield strength graduation as the final one, but without isostatic adjustment, produced a volume of 481,000 km^3, a figure very similar to that produced by Hulton et al. (2002).

The difference in reconstructed ice volumes between this study and Hollin and Schilling (1981) may reflect the setting of flow-lines, the yield strength applied for the ice-surface elevation calculation, and the topographic base used for each reconstruction. Our reconstruction here is based on connected flow-lines, from almost every glacially over-printed valley and based on a 100 m horizontal resolution base DEM, which were calculated with graduated yield strength values from 70 hPa to 130 hPa.

This compares to the Hollin and Schilling (1981) reconstruction which used a simplified bedrock geometry based on topographic W-E profiles each 40' and ice-surface profiles at each 2° of latitude, with a yield strength varying between 0 at the centre and 100 hPa at the margins. Apart from the different applications of yield strength values used, which has clear impact on reconstructed ice volume, Hollin and Schilling were unable to resolve strong topographic contrasts at that time, especially the deep fjords in the west.

The comparison between our LGM PIS reconstruction with the 'best-

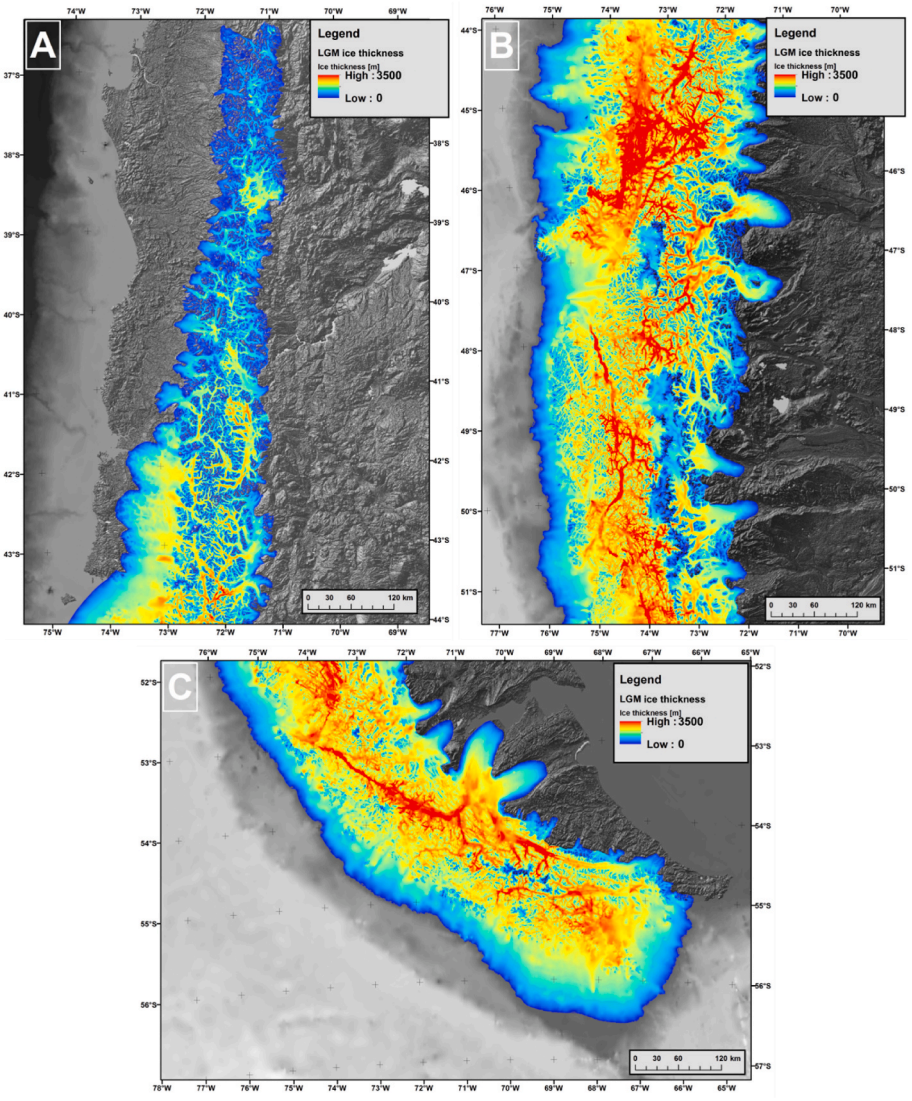

Fig. 4. Ice Sheet thickness maps for the reconstructed Patagonian Ice Sheet at the Last Glacial Maximum in areas A, B and C.

fit' LGM ice-sheet simulations by dynamic modelling (Hulton et al., 1994, 2002; Hulton and Sugden, 1997) reveal lower volume differences. The numerical model studies by Hulton et al. (1994, 2002); Hulton and Sugden (1997) used as boundary conditions the changing mass balance and topography interactions to simulate an LGM ice sheet with the closest fit to the LGM extents from Hollin and Schilling (1981) and Clapperton (1993). The first modelling attempts by Hulton et al. (1994); Hulton et al. (1994, 1997), Hulton et al. (1994) and Hulton and Sugden (1997) are based on the same model by Hulton et al. (1994) and were based on a topographic surface with a horizontal resolution of 20 km. This spatial resolution is 200 times coarser than the surface of the ice-sheet reconstruction used in our study. As a result, these first modelling attempts failed to reproduce any of the eastwards-flowing outlet lobes and the northern part of the LGM PIS is separated.

The later modelled LGM PIS by Hulton et al. (2002) and also used by Sugden et al. (2002) was based on a 10-km resolution topography, and uses the same modelling approach as that documented by Hulton et al. (1994). The climatic forcing of this model was more advanced than previous attempts and produced important insights regarding the role of potential shifts of the SWWB in driving ice sheet extent.

Hubbard et al. (2005) applied a range of ELA depressions in the area of the contemporary NPI to calibrate a time-dependent model with well-constrained outlet lobe margins. An ELA depression of 900m provided the closest fit to the known lateral limits of the PIS. Their simulated outlet lobes have a very steep inclined surface slope, especially at the Pacific margin similar to many contemporary ice sheets with calving margins. The Hubbard et al. (2005) model reproduces the two major outlet lobes of the eastern margin of the PIS. We argue that their model yields ice that is potentially too thick in the region of the Pueyrredón Lobe; the former ice surface is higher than a number of contemporary summits such as Sierra Colorada which Boex et al. (2013) suggest existed as nunataks during the LGM.

More recently, Yan et al. (2022) used a 1-km resolution ice sheet model to identify theclimate sensitivity of Patagonian glaciers and examine their responses to climatic change during the LGM. They used the Parallel Ice Sheet Model (PISM; version 1.2.1) a three dimensional, thermodynamically coupled, hybrid ice sheet model. They produced an ensemble comprising 21 PMIP models to argue that during the LGM Patagonia was colder and drier with a decrease in annual mean temperature and precipitation by ~4.7 C and 12%, respectively compared with the present day. They modelled an extensive LGM ice sheet (~387, 000 km^2) which almost completely covered the Patagonian Andes, drained by ice streams at the western margins and fast-flowing outlet glaciers to the east in line with many geomorphological assessments (e.g. Glasser and Jansson, 2008). The modelled ice sheet extent is sensitive to the parameter combinations employed in the model initiation,

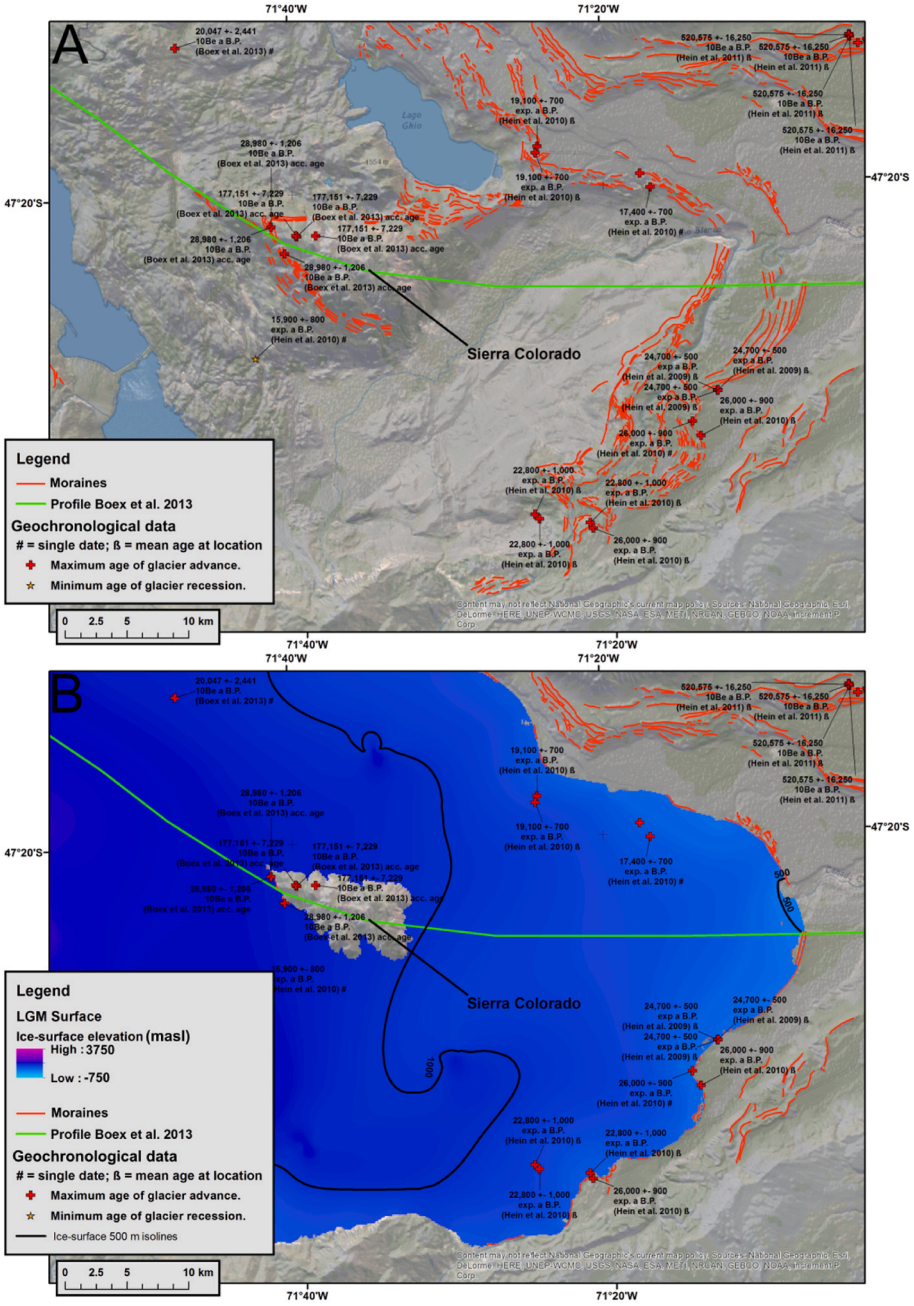

Fig. 5. Test of GIS-based reconstruction of the Patagonian Ice Sheet at the Last Glacial Maximum against previously constrained ice-surfaces in the Pueyrredón Lobe region (after Boex et al., 2013). Location of Figure is indicated on Fig. 1B. Panel A shows the general context, including mapped moraine limits and associated geochronology. Panel B shows the reconstructed LGM ice-surface elevation. Note that the pre-LGM dates obtained by Boex et al. (2013) at Sierra Colorada lie above the reconstructed LGM ice surface, which provides an independent test of the model.

Table 1
Reconstructions of the volume and sea level rise equivalents of the PIS from published papers.

Source	Ice Volume (km^3)	Sea level equivalent (m)
This study	554,067	1.38
This study (no isostatic adjustment)	481,252	1.12
Hollin and Schilling (1981)	340,000	0.85
Hulton et al. (1994); Hulton and Sugden (1997)	440,000	1.11
Hulton et al. (2002)	481,333	1.20
Davies et al. (2020) at 35ka	541,200	1.49
Davies et al. (2020) at 25ka	503,500	1.39

especially the positive degree-day factor for ice and annual temperature change and ranged from ~190,000 to 425,000 km^2. They did not assess the volume of the former PIS.

Our reconstruction of the LGM PIS therefore produces an extensive ice sheet with a slightly larger volume than any of the previous reconstructions. However, we cannot use this to assess the climate sensitivity of Patagonian glaciers as the degree of LGM cooling is still contested (see Tierney et al., 2020; Annan et al., 2022).

5. Conclusions

We present a new reconstruction of the PIS in order to refine earlier work (e.g. Hollin and Schillin, 1981; Hulton et al., 2002; Sugden et al., 2002). These early attempts were hampered by the coarse spatial resolution of basal topography (around 10 km). Our inverse-modelling approach requires a planform extent as well as a topographic dataset

and concentrates fully on the glacial geomorphological record of LGM limits.

We do not apply any climate scenarios to our reconstruction, although this could be used as a base data set for such initiatives. We argue that our reconstructed ice sheet produces the most accurate likely shape of the LGM PIS, scaling down to individual valleys. However, the inverse-modelling approach has limitations. The flow-line-based reconstruction approach can only deliver a static representation of an ice sheet on the basis of simplified physical laws within the planform limits and the given topography. While the flow-lines, topography, and the planform limits are fixed, yield strength values can be manipulated.

In addition, such reconstructions are unable to simulate the dynamics of calving margins, nor the role that deformable beds might have played in driving the evolution of the LGM ice sheet behaviour, especially to the east of the region. Nor is the likely ice sheet behaviour between the maritime west and continental east resolved. Finally, the only available ice thickness validation is at Lago Pueyrredón (Boex et al., 2013) and of course this may not be valid for the rest of the PIS. A full ice-sheet validation is only possible if more data on the 3D chronological evolution of the PIS becomes available.

Declaration of competing interest

A steady-state model reconstruction of the Patagonian Ice Sheet during the Last Glacial Maximum.

Data availability

Data will be made available on request.

Acknowledgements

A.H. gratefully acknowledges an Arctic Five Chair, funding from the Research Council of Norway through its Centres of Excellence scheme (CAGE & IC3 - Grants 223259 & 332635), The University of Oulu - Arctic Interactions and the Academy of Finland PROFI4 (Grant 318930).

References

Abram, N.J., Mulvaney, R., Vimeux, F., Phipps, S.J., Turner, J., England, M.H., 2014. Evolution of the southern annular Mode during the past millennium. Nat. Clim. Change 4 (7), 564.

Annan, J.D., Hargreaves, J.C., Mauritsen, T., 2022. A new global surface temperature reconstruction for the Last Glacial Maximum. Clim. Past 18, 1883–1896. https://doi.org/10.5194/cp-18-1883-2022.

Boex, J., Fogwill, C., Harrison, S., Glasser, N.F., Hein, A., Schnabel, C., Xu, S., 2013. Rapid thinning of the late Pleistocene patagonian ice sheet followed migration of the southern westerlies. Sci. Rep. 3, 1–6.

Caldenius, C.C., 1932. Las glaciaciones cuaternarias en la Patagonia y Tierra del Fuego. Geogr. Ann. 14, 1–164.

Clapperton, C.M., 1993. Nature of environmental changes in south America at the last glacial maximum. Palaeogeogr. Palaeoclimatol. Palaeoecol. 101, 189–208.

Coronato, A., Martínez, O., Rabassa, J., 2004. Glaciations in Argentine Patagonia, southern south America. Dev. Quat. Sci. 2, 49–67.

Davies, B.J., Darvill, C.M., Lovell, H., Bendle, J.M., Dowdeswell, J.A., Fabel, D., Gheorghiu, D.M., 2020. The evolution of the patagonian ice sheet from 35 ka to the present day (PATICE). Earth Sci. Rev. 204, 103152.

Darvill, C.M., Bentley, M.J., Stokes, C.R., Hein, A.S., Rodés, Á., 2015b. Extensive MIS 3 glaciation in southernmost Patagonia revealed by cosmogenic nuclide dating of outwash sediments. Earth Planet Sci. Lett. 429, 157–169.

Darvill, C.M., Bentley, M.J., Stokes, C.R., Shulmeister, J., 2016. The timing and cause of glacial advances in the southern mid-latitudes during the last glacial cycle based on a synthesis of exposure ages from Patagonia and New Zealand. Quat. Sci. Rev. 149, 200–214.

Denton, G.H., Hughes, T.J. (Eds.), 1981. The Last Great Ice Sheets, vol. 1. Wiley.

Denton, G.H., Lowell, T.V., Heusser, C.J., Schlüchter, C., Andersen, B.G., Heusser, L.E., Moreno, P.I., Marchant, D.R., 1999. Geomorphology, stratigraphy, and radiocarbon chronology of LlanquihueDrift in the area of the southern Lake District, seno reloncaví, and Isla grande de Chiloé, Chile. Geogr. Ann. Phys. Geogr. 81, 167–229.

García, J.L., Lüthgens, C., Vega, R.M., Rodés, Á., Hein, A.S., Binnie, S.A., 2021. A composite 10 Be, IR-50 and 14 C chronology of the pre-Last Glacial Maximum (LGM) full ice extent of the western Patagonian Ice Sheet on the Isla de Chiloé, south Chile (42° S). E&G Quaternary Science Journal 70 (1), 105–128.

Glasser, N.F., Harrison, S., Winchester, V., Aniya, M., 2004. Late Pleistocene and Holocene palaeoclimate and glacier fluctuations in Patagonia. Global Planet. Change 43 (1–2), 79–101.

Glasser, N.F., Jansson, K.N., 2005. Fast-flowing outlet glaciers of the last glacial maximum patagonian icefield. Quat. Res. 63, 206–211.

Glasser, N., Jansson, K., 2008. The glacial map of southern south America. J. Maps 4, 175–196.

Glasser, N.F., Jansson, K.N., Harrison, S., Kleman, J., 2008. The glacial geomorphology and Pleistocene history of South America between 38°S and 56°S. Quat. Sci. Rev. 27, 365–390.

Glasser, N.F., Harrison, S., Schnabel, C., Fabel, D., Jansson, K.N., 2012. Younger Dryas and early Holocene age glacier advances in Patagonia. Quat. Sci. Rev. 58, 7–17.

Gowan, E.J., Zhang, X., Khosravi, S., Rovere, A., Stocchi, P., Hughes, A.L., Gyllencreutz, R., Mangerud, J., Svendsen, J.I., Lohmann, G., 2021. A new global ice sheet reconstruction for the past 80 000 years. Nat. Commun. 12 (1), 1–9.

Hein, A.S., Hulton, N.R., Dunai, T.J., Schnabel, C., Kaplan, M.R., Naylor, M., Xu, S., 2009. Middle Pleistocene glaciation in Patagonia dated by cosmogenic-nuclide measurements on outwash gravels. Earth Planet Sci. Lett. 286 (1–2), 184–197.

Hein, A.S., Hulton, N.R., Dunai, T.J., Sugden, D.E., Kaplan, M.R., Xu, S., 2010. The chronology of the Last Glacial Maximum and deglacial events in central Argentine Patagonia. Quat. Sci. Rev. 29 (9–10), 1212–1227.

Heusser, C.J., 2003. Ice Age Southern Andes. Elsevier.

Hubbard, A.L., 1997. Modelling climate, topography and palaeoglacier fluctuations in the Chilean Andes. Earth Surf. Process. Landforms: The Journal of the British Geomorphological Group 22 (1), 79–92.

Hubbard, A., Hein, A.S., Kaplan, M.R., Hulton, N.R.J., Glasser, N., 2005. A modelling reconstruction of the last glacial maximum ice sheet and its deglaciation in the vicinity of the northern patagonian icefield, south America. Geogr. Ann. 87, 375–391.

Hughes, P.D., 2022. Concept and global context of the glacial landforms from the Last Glacial Maximum. In: European Glacial Landscapes. Elsevier, pp. 355–358.

Hughes, T.J., 1979. Reconstruction and disintegration of ice sheets for the CLIMAP 18000 and 125000 years BP experiments: theory. J. Glaciol. 24 (90), 493–495.

Hulton, N., Sugden, D., 1997. Dynamics of mountain ice caps during glacial cycles: the case of Patagonia. Ann. Glaciol. 24, 81–89.

Hulton, N.R., Sugden, D.E., Payne, A., Clapperton, C., 1994. Glacier modeling and the climate of Patagonia during the last glacial maximum. Quat. Res. 42, 1–19.

Hulton, N.R.J., Purves, R.S., McCulloch, R.D., Sugden, D.E., Bentley, M.J., 2002. The last glacial maximum and deglaciation in southern south America. Quat. Sci. Rev. 21, 233–241.

Jones, J.M., Gille, S.T., Goosse, H., Abram, N.J., Canziani, P.O., Charman, D.J., Clem, K. R., Crosta, X., De Lavergne, C., Eisenman, I., England, M.H., 2016. Assessing recent trends in high-latitude Southern Hemisphere surface climate. Nat. Clim. Change 6 (10), 917.

Kaplan, M.R., Fogwill, C.J., Sugden, D.E., Hulton, N.R.J., Kubik, P.W., Freeman, S.P.H.T., 2008. Southern patagonian glacial chronology for the last glacial period and implications for southern ocean climate. Quat. Sci. Rev. 27, 284–294.

Kaplan, M.R., Hein, A.S., Hubbard, A., Lax, S.M., 2009. Can glacial erosion limit the extent of glaciation? Geomorphology 103 (2), 172–179.

Kilian, R., Lamy, F., 2012. A review of Glacial and Holocene paleoclimate records from southernmost Patagonia (49–55°S). Quat. Sci. Rev. 53, 1–23.

Lenaerts, J.T., Van Den Broeke, M.R., van Wessem, J.M., van de Berg, W.J., van Meijgaard, E., van Ulft, L.H., Schaefer, M., 2014. Extreme precipitation and climate gradients in Patagonia revealed by high-resolution regional atmospheric climate modeling. J. Clim. 27, 4607–4621.

Leger, T.P.M., Hein, A.S., Bingham, R.G., Rodés, A., Fabel, D., Smedley, R.K., 2021. Geomorphology and 10 Be chronology of the last glacial maximum and deglaciation in northeastern Patagonia, 43°S- 71°W. Quat. Sci. Rev. 272, 107194.

McCulloch, R.D., Bentley, M.J., Purves, R.S., Hulton, N.R.J., Sugden, D.E., Clapperton, C. M., 2000. Climatic inferences from glacial and palaeoecological evidence at the last glacial termination, southern South America. J. Quat. Sci. 15, 409–417.

Nye, J.F., 1952a. The mechanics of glacier flow. J. Glaciol. 2 (12), 82–93.

Nye, J.F., 1952b. A comparison between the theoretical and the measured long profile of the Unteraar glacier. J. Glaciol. 2 (No. 12), 103–107.

Nye, J.F., 1957. The distribution of stress and velocity in glaciers and ice-sheets. Proc. Roy. Soc. Lond. Math. Phys. Sci. 239 (1216), 113–133.

Rabassa, J., Coronato, A.M., Salemme, M., 2005. Chronology of the Late Cenozoic Patagonian glaciations and their correlation with biostratigraphic units of the Pampean region (Argentina). J. S. Am. Earth Sci. 20 (1–2), 81–103.

Rabassa, J., 2008. Late Cenozoic glaciations in Patagonia and Tierra del Fuego. Dev. Quat. Sci. 11, 151–204.

Schilling, D., Hollin, J., 1981. Numerical reconstructions of valley glaciers and small ice caps. In: Denton, G., Hughes, T. (Eds.), The Last Great Ice Sheets. Wiley-Interscience, pp. 207–220. Ch. 4.

Sejrup, H.P., Hjelstuen, B.O., Patton, H., Esteves, M., Winsborrow, M., Rasmussen, T.L., Andreassen, K., Hubbard, A., 2022. The role of ocean and atmospheric dynamics in the marine-based collapse of the last Eurasian Ice Sheet. Communications Earth & Environment 3 (1), 1–10.

Sherwood, S., Webb, M.J., Annan, J.D., Armour, K., Forster, P.M., Hargreaves, J.C., Hegerl, G., Klein, S.A., Marvel, K.D., Rohling, E.J., Watanabe, M., Andrews, T., Braconnot, P., Bretherton, C.S., Foster, G.L., Hausfather, Z., von der Heydt, A.S., Knutti, R., Mauritsen, T., Norris, J.R., Proistosescu, C., Rugenstein, M., Schmidt, G. A., Tokarska, K.B., Zelinka, M.D., 2020. An assessment of Earth's climate sensitivity using multiple lines of evidence. Rev. Geophys. 58, e2019RG000678.

Soteres, R.L., Sagredo, E.A., Kaplan, M.R., et al., 2022. Glacier fluctuations in the northern Patagonian Andes (44°S) imply wind-modulated interhemispheric in-phase

climate shifts during Termination 1. Sci Rep 12, 10842. https://doi.org/10.1038/s41598-022-14921-4Soteres.

Sugden, D. E., Hulton, N. R., & Purves, R. S. (2002). Modelling the inception of the Patagonian icesheet. *Quaternary International*, *95*, 55-64.Sugden, D.E., Hulton, N.R., Purves, R.S., 2002. Modelling the inception of the Patagonian icesheet. Quat. Int. 95, 55e64.

Sugden, D.E., Bentley, M.J., Fogwill, C.J., Hulton, N.R.J., McCulloch, R.D., Purves, R.S., 2005. Late-glacial glacier events in southernmost South America: a blend of 'Northern' and 'Southern' hemispheric climate signals? Geogr. Ann. Phys. Geogr. 87, 273–288.

Tierney, J.E., Zhu, J., King, J., Malevich, S.B., Hakim, G.J., Poulsen, C.J., 2020. Glacial cooling and climate sensitivity revisited. Nature 584 (7822), 569–573.

Warren, C.R., Sugden, D.E., 1993. The Patagonian icefields: a glaciological review. Arct. Alp. Res. 25 (4), 316–331.

Wenzens, G., 2005. Glacier Advances East of the Southern Andes between the Last Glacial Maximum and 5,000 BP Compared with Lake Terraces of the Endorrheic Lago Cardiel (49 S, Patagonia, Argentina). Zeitschrift für Geomorphologie, NF, pp. 433–454.

Wenzens, G., 2006. Terminal moraines, outwash plains, and lake terraces in the vicinity of Lago cardiel (49°S; Patagonia, Argentina)—evidence for miocene andean foreland glaciations. Arctic Antarct. Alpine Res. 38, 276–291.

Wolff, I.W., 2016. The Last Glacial Maximum Patagonian Ice Sheet: A GIS Based Reconstruction Approach. PhD Thesis. Aberystwyth University.

Wolff, I.W., Glasser, N.F., Hubbard, A., 2013. The reconstruction and climatic implication of an independent palaeo ice cap within the Andean rain shadow east of the former Patagonian ice sheet, Santa Cruz Province, Argentina. Geomorphology 185, 1–15.

Yan, Q., Wei, T., Zhang, Z., 2022. Modeling the climate sensitivity of Patagonian glaciers and their responses to climatic change during the global last glacial maximum. Quat. Sci. Rev. 288, 107582.